Remote Sensing of Environment 326 (2025) 114818

Contents lists available at ScienceDirect

Remote Sensing of Environment

journal homepage: www.elsevier.com/locate/rse

Leveraging transfer learning and leaf spectroscopy for leaf trait prediction with broad spatial, species, and temporal applicability

Fujiang Ji [a], Fa Li [a], Hamid Dashti [a], Dalei Hao [b], Philip A. Townsend [a], Ting Zheng [a], Hangkai You [a], Min Chen [a,c,*]

[a] Department of Forest and Wildlife Ecology, University of Wisconsin-Madison, 1630 Linden Drive, Madison, WI 53706, USA
[b] Atmospheric, Climate, and Earth Sciences Division, Pacific Northwest National Laboratory, 902 Battelle Blvd, Richland, WA 99354, USA
[c] Data Science Institute, University of Wisconsin-Madison, 447 Lorch Ct, Madison, 53706, WI, USA

ARTICLE INFO

Edited by: Jing M. Chen

Keywords:
Leaf traits
Model transferability
Machine learning
Radiative transfer models

ABSTRACT

Accurate and reliable prediction of leaf traits is crucial for understanding plant adaptations to environmental variation, monitoring terrestrial ecosystems, and enhancing comprehension of functional diversity and ecosystem functioning. Currently, various approaches (e.g., statistical, physical models) have been developed to estimate leaf traits through hyperspectral remote sensing and leaf spectroscopy. However, the absence of high-performing, transferable, and stable models across various domains of space, plant functional types (PFTs) and seasons hinder our ability to quantify and comprehend spatiotemporal variations in leaf traits. This study proposes robust and highly transferable models for better predicting leaf traits with hyperspectral reflectance. Initially, three datasets were assembled, pairing common leaf traits — chlorophyll (Chla+b), carotenoids (Ccar), leaf mass per area (LAM), equivalent water thickness (EWT) — with leaf spectra measurements collected across diverse geographic locations in the U.S. and Europe, PFTs, and seasons. Measurements were acquired using spectroradiometers (e.g., ASD FieldSpec 3/4/Pro and SVC HR-1024i) with integrating spheres, leaf clips, and contact probes. We then developed transfer learning-based hybrid models that incorporated the domain knowledge of radiative transfer models (RTMs) through pretraining processes and were well-constrained by fine-tuning with field measurements. Through comparison with other state-of-the-art statistical models, including partial-least squares regression (PLSR) and Gaussian Process Regression (GPR), as well as pure physical models, we found that the proposed transfer learning models achieved better predictive performance and higher transferability. Specifically, compared to other statistical models and pure RTMs, the transfer learning model exhibited higher coefficient of determination (R^2) values with range of 0.01 to 0.79, lower normalized root mean square error (NRMSE) with range of 0.06 % to 33.25 % in model performance. Additionally, the models exhibited improved transferability, with higher R^2 values range from 0.04 to 0.32, lower NRMSE range from 0.08 % to 30.81 %. The findings underscore that transfer learning models through integrating domain knowledge from RTMs and limited observations, can harness the advantages of both RTMs and statistical models and serve as a promising approach for effectively predicting leaf traits.

1. Introduction

Accurate quantification of leaf traits is crucial for understanding plant adaptation (Adler et al., 2013; Fajardo and Siefert, 2016), ecosystem functioning (Asner and Martin, 2016) and interactions with their environment. These traits provide insights into resource strategies (Collins et al., 2016; Vendramini et al., 2002), nutrient cycling, and productivity (Schimel et al., 2019; Van Bodegom et al., 2014), supporting Earth system models (Fatichi et al., 2019; Rogers et al., 2017; Skidmore et al., 2021) for better predicting ecosystem responses to climate change (Ito et al., 2006; Reichstein et al., 2014). Despite global trait databases being larger and more accessible than ever, significant gaps and sampling biases still hinder trait-based ecological research (Cornwell et al., 2019; Kattge et al., 2020), and efforts to upscale traits spatially from databases remain challenged by those gaps (Dechant et al., 2024). Traditional wet chemical analysis methods are cost- and

* Corresponding author at Department of Forest and Wildlife Ecology, University of Wisconsin-Madison, 1630 Linden Drive, Madison, WI, USA.
E-mail address: min.chen@wisc.edu (M. Chen).

https://doi.org/10.1016/j.rse.2025.114818
Received 1 December 2024; Received in revised form 30 April 2025; Accepted 10 May 2025
Available online 20 May 2025
0034-4257/© 2025 Elsevier Inc. All rights are reserved, including those for text and data mining, AI training, and similar technologies.

labor-intensive (Burnett et al., 2021; McKown et al., 2013; Szollosi et al., 2011). Leaf spectroscopy, however, offers powerful opportunities to estimate leaf traits from their optical properties, filling these gaps and improving ecosystem monitoring and management (Hill et al., 2019; Nakaji et al., 2019; Serbin et al., 2019; Spafford et al., 2021; Yan et al., 2021; Yang et al., 2016).

The widely used spectroscopy-based leaf trait estimation method relies on vegetation indices (VIs) to infer leaf traits (Schlemmera et al., 2013; Xu et al., 2019). VI-based methods are particularly suitable for multispectral data and can achieve acceptable estimations but often lack robustness due to uncertainty in VI-trait relationships and saturation effects, which limit their broad application (Colombo et al., 2008; Zeng et al., 2022). In contrast, multivariate statistical methods like partial least square regression (PLSR. Wold et al., 1984) and machine learning (ML) algorithms such as deep neural networks (DNNs) (Hornik et al., 1989; Shabani et al., 2017) and GPR (Rasmussen, 2004) have been commonly used for leaf trait estimation. These approaches leverage the higher spectral dimensionality of hyperspectral data, enabling more comprehensive analyses by utilizing the full spectral information, which is less feasible with the VI-based methods. Recent developments include more complex machine-learning models, such as multi-trait 1-D convolutional neural networks (CNN) models (Cherif et al., 2023), which outperform PLSR models but require large, often costly and unavailable training datasets. In general, multivariate statistical methods make full use of the hyperspectral information and usually perform well within the training space but can lose generalizability when applied to new measurements out of the range of the data used to train the predictive models, as we shown in previous study with a comprehensive dataset (Ji et al., 2024). In parallel, physical models, also known as radiative transfer models (RTMs) are widely used. Notable examples include the PROSPECT model (Jacquemoud and Baret, 1990) and the Leaf-SIP model (Wu et al., 2021). These models are developed upon physical interpretation of the interaction between electromagnetic radiation and leaf constituents. They are typically considered more robust and transferable than statistical models (Jacquemoud et al., 2009), but have been criticized for their relatively poor predictive accuracy (Verrelst et al., 2019; Wang et al., 2021, 2015) as well as for the "ill-posed" problem widely existing in RTM inversions that different trait combinations yield similar reflectance (Combal et al., 2003; Lewis and Disney, 2007).

More recently, the hybrid models have been developed to address the challenges of previous methods, combining the physical basis of RTMs with the efficiency and flexibility of regression methods. These models train machine learning algorithms on synthetic data simulated by RTMs, leveraging the causal relationships between RTM inputs (e.g. leaf traits) and outputs (e.g. leaf optics) (Doktor et al., 2014; Verger et al., 2011). However, RTMs themselves can be biased and have low predictive accuracy and the ML model trained on them is consequently biased with poor performance on real data. Alternatively, transfer learning techniques provide potential solutions that make full use of process-model generated synthetic data as compensation to limited sample sizes to address the unknown physics simplification in RTMs (Berger et al., 2018; Reichstein et al., 2019; Verrelst et al., 2019; Wang et al., 2021; Yuan et al., 2022; Zhu et al., 2022).

Transfer learning techniques can be categorized into five types: fine-tuning-based transfer learning, multi-task learning, few-shot learning, unsupervised domain adaptation, and self-supervised learning (Ma et al., 2024). These approaches have been applied to various research areas, including land cover mapping (de Lima and Marfurt, 2019; Nowakowski et al., 2021), soil property estimation (Shen et al., 2022) and crop yield prediction (Zhao et al., 2022). In plant trait estimation, several studies have demonstrated the potential of transfer learning. Wang et al. (2023b) developed a process-guided machine learning model that outperforms traditional methods in estimating crop traits. Wan et al. (2022) utilized a transfer learning model, TCA-SVR, that showed a greater performance than PLSR model in predicting leaf nitrogen content and improved model transferability across 5 spectra-trait datasets. Zhang et al. (2021) used the fine-tuning-based transfer learning methods to estimate leaf chlorophyll content and improved the model accuracy and transferability across two closed fields. While these studies, focused on specific small regions or species, have shown transfer learning's capability to enhance leaf trait estimation models, the broader applicability and transferability of these models remain unknown. A truly effective predictive model should be transferable across different dimensions such as spatial scales, species, and time periods, given the complexity of natural systems.

The objective of this study is to develop this kind of model for estimating leaf traits and evaluate its accuracy and transferability. Developing robust and highly transferable models that can infer leaf traits across different locations, species, and time simultaneously is essential and timely, particularly in the context of current and upcoming global satellite imaging spectroscopy missions like ESA's Copernicus Hyperspectral Imaging Mission for the Environment (CHIME, Nieke and Rast, 2018) and NASA's Surface Biology and Geology (SBG, Cawse-Nicholson et al., 2021). We present two main questions: (1) Do our proposed transfer learning models for predicting leaf traits have better performance than other state-of-the-art statistical models like PLSR and GPR, and the pure RTMs? (2) Are the transfer learning models more transferable across different geographic locations, plant functional types (PFTs), and seasons than other models? (3) How the inconsistency and the quantity of real observations used for fine-tuning influence the performance of transfer learning models?

2. Materials and methods

2.1. Leaf traits and leaf spectra measurements

We used a large dataset compiled by Ji et al. (2024) that paired a variety of leaf traits with leaf spectra measurements with 47,393 samples, over 700 species, and 101 locations distributed over multiple continents. To evaluate the performance and robustness of the developed models, we created three distinct subsets (spatial, PFT and temporal) from the compiled dataset (Fig. 1 and Table 1). In the spatial and PFT datasets, leaf spectra were measured using two different spectroradiometers: the ASD FieldSpec 3/4/Pro (Malvern Analytical Inc., Westborough, MA, USA) for Chla+b, Ccar, and LMA samples, and the SVC HR-1024i full-spectrum spectroradiometer (Spectra Vista Corp., Poughkeepsie, NY, USA) for EWT samples. In the temporal dataset, all spectra were measured using the ASD FieldSpec 3/4/Pro. Moreover, three measurement methods were used, an integrating sphere, which captured spectra as directional-hemispherical reflectance (DHRF); and a leaf clip and contact probe, which acquired spectra as bidirectional reflectance factor (BRF). Detailed information on the spectral measurements is provided in Table 1.

To ensure the consistent spectral resolution, all leaf spectra were subsampled to 10 nm intervals using the resampling method described by Adjorlolo et al. (2013) and Fu et al. (2020). For each band center, a Gaussian model with a full width at half maximum (FWHM) equivalent to the specified bandwidth interval (10 nm) was applied to convolve the original reflectance spectra, effectively simulating the spectral resolution of the data. The analysis specifically focused on wavelengths ranging from 450 nm to 2400 nm. Additionally, we ensured a relatively balanced representation of leaf samples across various sites, PFTs, and seasons by randomly selecting samples to achieve equal or approximately equal representation for each category. For example, in the spatial dataset, we included a total of 1600 Chla+b samples evenly distributed across eight sites in the U.S. and Europe, with 200 samples per site. For Ccar, there were 1000 samples from five sites, with 200 samples per site. The EWT dataset consisted of 400 samples from four sites, with 100 samples per site, while the LMA dataset included 4800 samples from twelve sites, with 400 samples per site (Fig. 1 and Table 1). A similar sampling strategy was applied to the PFT and temporal datasets (Table 1). This sampling strategy mitigates potential biases and

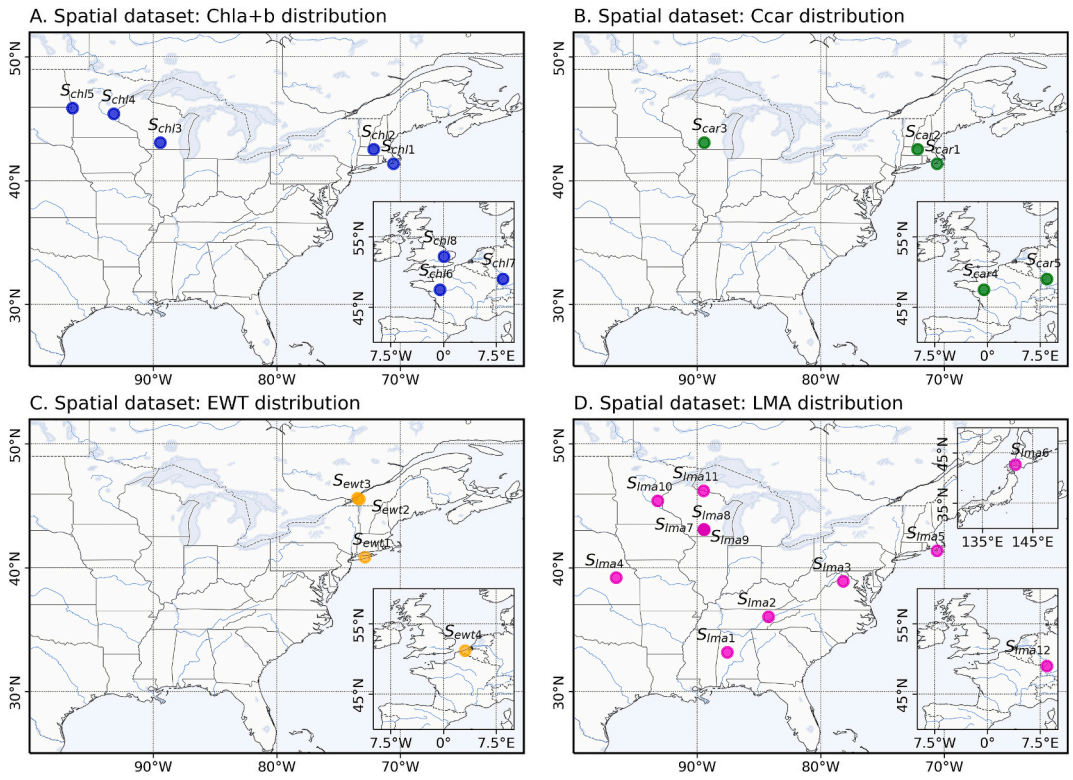

Fig. 1. Spatial distribution of leaf trait samples in the spatial dataset. A. Chla+b samples distribution, B. Ccar samples distribution, C. EWT samples distribution and D. LMA samples distribution. S_{chl1} to S_{chl8}, S_{car1} to S_{car5}, S_{ewt1} to S_{ewt4} and S_{lma1} to S_{lma12} represent the site numbers of Chla+b, Ccar, EWT and LMA, respectively. Chla+b, Ccar, EWT and LMA correspond to chlorophyll contents, carotenoid contents, equivalent water thickness and leaf mass per area, respectively.

ensures fairness in the subsequent cross-validation procedures and guarantees that variations in model accuracy will not be influenced by disparities in the number of training or validation samples. The samples in the temporal dataset are located in the temperate northern hemisphere and share the same PFT (DBF).

2.2. Modeling methods

To develop robust and transferable models for predicting leaf traits, we designed the framework with the following four steps (Fig. 2.).

Step I: Pure radiative transfer modeling. We applied two RTMs rooted in different principles, PROSPECT-D (Jacquemoud and Baret, 1990) and Leaf-SIP (Wu et al., 2021). PROSPECT employs the generalized plate model, which simulates leaf optical properties over the spectral domain from 400 to 2500 nm with 1 nm spectral resolution based on the light-absorbing biochemical constituents like chlorophyll, carotenoids, equivalent water thickness and leaf mass per area, etc., the corresponding pigments absorption coefficients, as well as a spectral refractive index and leaf mesophyll structure parameter N. The leaf-SIP model draws from spectral invariants theory (Knyazikhin et al., 1998; Stenberg et al., 2016), which decouples the leaf scale radiative transfer process into two parts: the wavelength-dependent contribution from leaf chemical components and wavelength-independent contribution from leaf structures, described by two spectrally invariant parameters, a photon recollision probability p and a scattering asymmetry parameter q. The inversion processes of radiative transfer models were based on an iterative optimization method (differential evolution; Storn and Price, 1997), which minimize the residuals between measured and modeled leaf reflectance using a *RMSE*-based cost function over the full spectral ranges by exploring the boundary predefined input parameter space of the model.

Step II: Transfer learning modeling. We combined the radiative transfer models described in the first step and observational data with several fine-tuning strategies to build the transfer learning models for leaf trait estimation. In particular, we first ran RTMs in forward mode to simulate a synthetic dataset comprising 10,000 pairs of synthetic leaf spectra and leaf traits (Herman and Usher, 2017). The range of model input parameters for generating this dataset was shown in Table 2. These ranges were determined based on a combination of trait value ranges observed in the dataset and values reported in previous studies (Berger et al., 2020; Féret et al., 2017; Jay et al., 2016; Jiang et al., 2021; Wan et al., 2021). Subsequently, this simulated synthetic data was randomly split into 90 % for calibration and 10 % for validation, which were employed to construct individual pre-trained DNN models for each leaf trait. The pre-trained DNN models were built using the PyTorch API, featuring a three-layer fully connected network. The hidden layers consisted of 196, 64, and 32 nodes, each employing the ReLU activation function. The training process involved using the Adam optimizer, optimizing with the L1 Loss function, and running for 300 epochs. Crucial hyperparameters such as learning rate and batch size were determined through GridSearchCV method (Bergstra et al., 2012). Finally, we applied four fine-tuning strategies to build the transfer learning models, namely, random fine-tuning, spatial fine-tuning, cross-PFTs fine-tuning, and temporal fine-tuning. The fine-tuning refers to the process of updating the parameters of pre-trained DNN models with new observational data to better adapt them to specific applications. Random fine-tuning involved randomly selecting varying portions of observational data (10 %, 20 %, …, 80 %) as the calibration sets, repeated 10 times for each portion, to fine-tune pre-trained DNN models and the rest of the observations were used for model validation. Spatial fine-tuning iteratively utilized all data in spatial dataset except that from a single site as calibration set while keeping the remaining one site data as the validation set. Within each calibration set, we further randomly divided the data into 80 % and 20 % splits, repeating this process 10 times for pre-trained model fine-tuning. The performance of each iteration was assessed using the excluded site, and the average performance and

Table 1
Description of the datasets. CRP, GRA, DBF, EBF, ENF, Vine and SHR refer to croplands, grasslands, deciduous broadleaf forests, evergreen broadleaf forests, evergreen needleleaf forests, vine and shrublands, respectively. Chla+b, Ccar, EWT and LMA correspond to chlorophyll contents, carotenoid contents, equivalent water thickness and leaf mass per area, respectively.

Leaf traits/datasets	Spectrora-diometers	Spatial dataset	PFT dataset	Temporal dataset
Chla+b ($\mu g/cm^2$)	ASD FieldSpec 3/ 4/Pro	o **1600** samples. 8 sites (200 samples for each site). o Foreoptic type: integrating sphere, leaf clip, and contact probe.	o **3000** samples. DBF, CPR, GRA (1000 samples for each PFT). o Foreoptic type: integrating sphere, leaf clip, and contact probe.	o **608** samples. o Early growing season (71 samples); o Peak growing season (278 samples); o Post-peak season (259 samples) o Foreoptic type: integrating sphere.
Ccar ($\mu g/cm^2$)	ASD FieldSpec 3/ 4/Pro	o **1000** samples. 5 sites (200 samples for each site). o Foreoptic type: integrating sphere, leaf clip.	o **2100** samples. DBF, CPR and GRA (700 samples for each PFT). o Foreoptic type: integrating sphere, leaf clip, contact probe.	o **634** samples. o Early growing season (71 samples); o Peak growing season (278 samples); o Post-peak season (285 samples) o Foreoptic type: integrating sphere.
EWT (g/m^2)	SVC HR-1024i	o **400** samples. 4 sites (100 samples for each site). o Foreoptic type: integrating sphere, leaf clip.	o **540** samples. DBF, GRA, CPR (180 samples for each PFT). o Foreoptic type: integrating sphere, leaf clip.	N/A
LMA (g/m^2)	ASD FieldSpec 3/ 4/Pro	o **4800** samples. 12 sites (400 samples for each site). o Foreoptic type: integrating sphere, leaf clip, and contact probe.	o **1400** samples. DBF, SHR, GRA, Vine, EBF, CPR and ENF (200 samples for each PFT). o Foreoptic type: integrating sphere, leaf clip, and contact probe.	o **626** samples. o Early growing season (278 samples); o Peak growing season (303 samples); o Post-peak season (45 samples) o Foreoptic type: integrating sphere.

uncertainties of these 10 models represented each iteration's outcome. The performance of the final model and associated uncertainties were determined by averaging across all iterations. Similarly, the cross-PFTs and temporal fine-tuning processes followed a comparable approach, which iteratively utilized all data in the PFT/temporal dataset except that from a single PFT/season as the calibration set while keeping the remaining one PFT/ season as the validation set. This was followed by employing analogous modeling strategies to those used in spatial fine-tuning. To enhance performance during the fine-tuning processes, we employed GridsearchCV to pinpoint the optimal hyperparameters such as initial learning rate and batch size, which helps us to achieve better performance and faster convergence.

Step III: Statistical modeling. We employed GPR and PLSR methods to estimate leaf traits. GPR is a nonlinear nonparametric machine learning algorithm that has gained increasing usage for trait estimation (Wang et al., 2019). GPR entails a probabilistic (Bayesian) approach for learning generic regression with kernels (Rasmussen, 2004). The output values of all training/testing data points are considered to be samples of a joint multivariate normal distribution, with the mean of a zero vector and the covariance matrix given by the kernel function. PLSR is a widely used multivariate linear regression for leaf trait estimation with leaf spectroscopy (Asner and Martin, 2008; Dechant et al., 2017; Townsend et al., 2003; Verrelst et al., 2019; Wold et al., 1984; Yendrek et al., 2017) and can effectively solve the multicollinearity problem of hyperspectral reflectance as it transforms input and target variables into several orthogonal latent vectors (Wold et al., 2001; Wold et al., 1984). In this study, The GPR models were implemented using the GPyTorch API, employing a constant mean and a radial basis function (RBF) kernel as their foundational components. These models were optimized using the Adam optimizer alongside exact marginal log-likelihood, focusing on minimizing the negative log-likelihood loss during the training process. PLSR models were built using the Python PLSRegression API. The optimal number of PLSR components was determined following Ji et al. (2024), in which iterative permutation is used to select the number of components that minimize the prediction residual error sum of squares (PRESS) (Allen, 1974; Allen, 1971). The training for statistical models followed the four strategies described for transfer learning fine-tuning processes in Step II.

Step IV: To assess the performance of the developed transfer learning models to predict leaf traits, we compared the results to state-of-the-art leaf trait prediction models, including GPR, PLSR, and pure RTMs (Section 2.3).

2.3. Statistical analysis and model evaluation

Mean values, standard deviations, the range of leaf traits and two-way analysis of variance (ANOVA) were employed to identify variations in traits across sites, PFTs, and seasons within the compiled datasets. The performance assessment of different models for estimating leaf traits was evaluated by standard summary statistics including coefficient of determination (R^2), root mean square error (*RMSE*) and normalized root mean square error (*NRMSE*, calculated by the *RMSE* divided by the range of the estimated leaf traits). Averaged accuracy was used to assess the performance of different models in predicting the selected leaf traits, based on averaging the accuracy for each individual trait. Out-of-domain accuracy was used to quantify the transferability of models, providing a metric of model performance when confronted with data from domains not represented in the training set.

3. Results

3.1. Variations of leaf traits and leaf spectra data

Leaf traits exhibited large variations across different sites, PFTs and

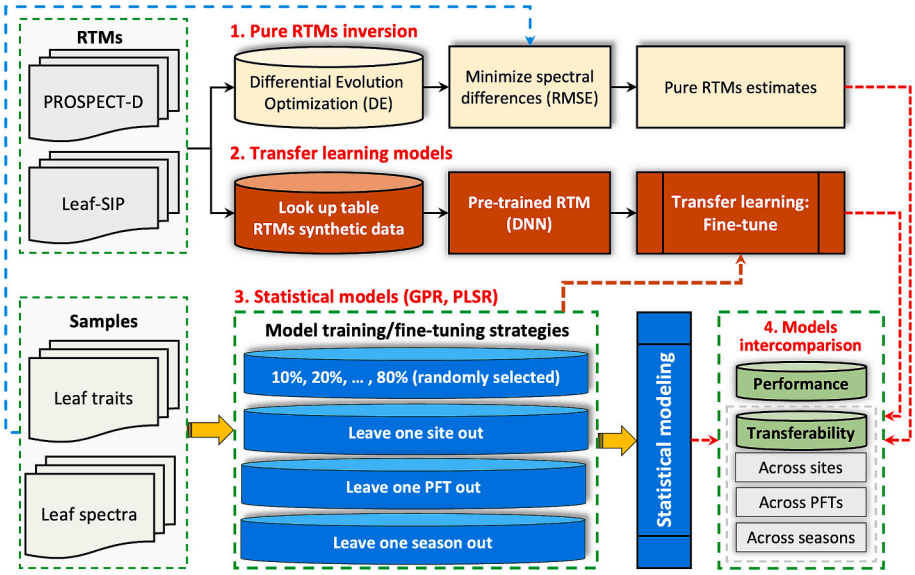

Fig. 2. Overall workflow for estimating leaf traits based on various models.

Table 2
Ranges of radiative transfer models (RTMs) input parameters for simulation synthetic data.

Model	Variable	Description	Unit	Range
PROSPECT-D	N	Leaf structural parameter	N/A	0.8-2.5
PROSPECT-D/Leaf-SIP	Chla+b	Leaf total chlorophyll content	μg/cm^2	0-170
PROSPECT-D/Leaf-SIP	Ccar	Leaf carotenoid content	μg/cm^2	0-30
PROSPECT-D/Leaf-SIP	Cbrw	Brown pigment content	μg/cm^2	0-1
PROSPECT-D/Leaf-SIP	EWT	Equivalent water thickness	g/m^2	20-1400
PROSPECT-D/Leaf-SIP	LMA	Leaf mass per area	g/m^2	0-400
PROSPECT-D/Leaf-SIP	Cant	Leaf anthocyanin content	μg/cm^2	0-10

seasons (Fig. 3 and Table S1). In the spatial dataset, site S_{chl1} have the highest values, which ranges from 1.43 to 59.94 μg/cm^2 with a mean value of 34.38 μg/cm^2 and a standard deviation of 13.15 μg/cm^2, while site S_{chl8} have the lowest values, which ranges from 3.48 to 23.91 μg/cm^2 with a mean value of 11.01 μg/cm^2 and a standard deviation of 4.98 μg/cm^2. Sites S_{car5} and S_{car2} displayed the largest and lowest values, with rages of 5.72-12.41 μg/cm^2 (mean ± 1std of 9.29 ± 1.71 μg/cm^2) and 1.7-9.58 μg/cm^2 (mean ± 1std of 5.48 ± 1.82 μg/cm^2), respectively. Sites S_{ewt4} and S_{ewt2} showed the largest and lowest values, spanning 70.1-477.02 g/m^2 (mean ± 1std of 187.98 ± 86.37 g/m^2) and 44.33-115.5 g/m^2 (mean ± 1std of 81.96 ± 17.54 g/m^2). Lastly, LMA samples demonstrated site S_{lma5} with the highest value, ranging from 59.65 to 254.39 g/m^2 with mean ± 1std of 137 ± 41.16 g/m^2) and S_{lma9} with the narrowest range (0.07-74.11 g/m^2, mean ± 1std of 32.1 ± 15.94 g/m^2). Among PFTs, croplands (CRP) exhibit the highest mean values for Chla+b, grasslands (GRA) exhibits the highest mean values for Ccar, and EWT, while evergreen needleleaf forests (ENF) stands out with the highest mean values for LMA. Moreover, all leaf traits in the temporal dataset, which are located in the temperate northern hemisphere, displayed strong seasonal variability. Chla+b and Ccar experience rapid increases during the early growing season, stabilizing at the peak growing season, and subsequently decline in post-peak season. LMA demonstrates an upward trend from the early growing season, with a gradual increases until leveling off at the end of the time series. The ANOVA test also indicated significant differences in leaf traits across sites, PFTs and seasons ($p < 0.001$) in the three compiled datasets.

Similarly, leaf reflectance and its coefficient of variation (CV) also displayed significant variations across sites, PFTs, and seasons, varying notably across different wavelength regions (Fig. 3, Table S2). Specifically, the reflectance variability in the visible (VIS: 450–750 nm), shortwave infrared 1 (SWIR1: 1300–1800 nm), and shortwave infrared 2 (SWIR2: 1800–2400 nm) bands was highest in SHR with CV values of 0.699 ± 0.267, 0.581 ± 0.178, and 1.078 ± 0.576, respectively, and ENF with CV values of 0.673 ± 0.257, 0.506 ± 0.160, and 0.918 ± 0.501, respectively. In contrast, the lowest variability was observed in CRP (CV = 0.312 ± 0.140, 0.081 ± 0.021, and 0.136 ± 0.027, respectively) and vine (CV = 0.215 ± 0.063, 0.081 ± 0.021, and 0.177 ± 0.053, respectively). Among phenological stages, the post-peak season exhibited the highest variability in the VIS and SWIR2 bands, with CV values of 0.418 ± 0.219 and 0.305 ± 0.103, respectively. Additionally, the early growing season demonstrated relatively higher variability than other stages in SWIR1 band, with a CV of 0.181 ± 0.017.

3.2. Leaf trait prediction

3.2.1. Synthetic and data pre-training

Fig. 4A illustrates the simulated synthetic reflectance generated using sampled leaf traits (Table 2) through the PROSPECT and Leaf-SIP models. Notably, the synthetic reflectance of the Leaf-SIP model was consistently higher than that of the PROSPECT model due to structural differences between the two models, particularly how they simulate the interactions between light and leaf tissues. These differences were also pronounced in the visible region (400–700 nm), which is critical for pigment-related absorption, and may therefore influence the estimation of pigments. Using these reflectance simulations, pre-trained DNN models were applied to predict leaf traits, with the results shown in Fig. 4B and Fig. 4C. These results demonstrate that the pre-trained DNN models effectively estimated the leaf traits when compared to their true values, regardless of whether the synthetic data were generated using PROSPECT or Leaf-SIP. For DNN models pre-trained with PROSPECT-generated synthetic data, the R^2 values are 1.0 for Chla+b, 0.96 for Ccar, 1.0 for EWT and 1.0 for LMA estimation, with *NRMSE* values of

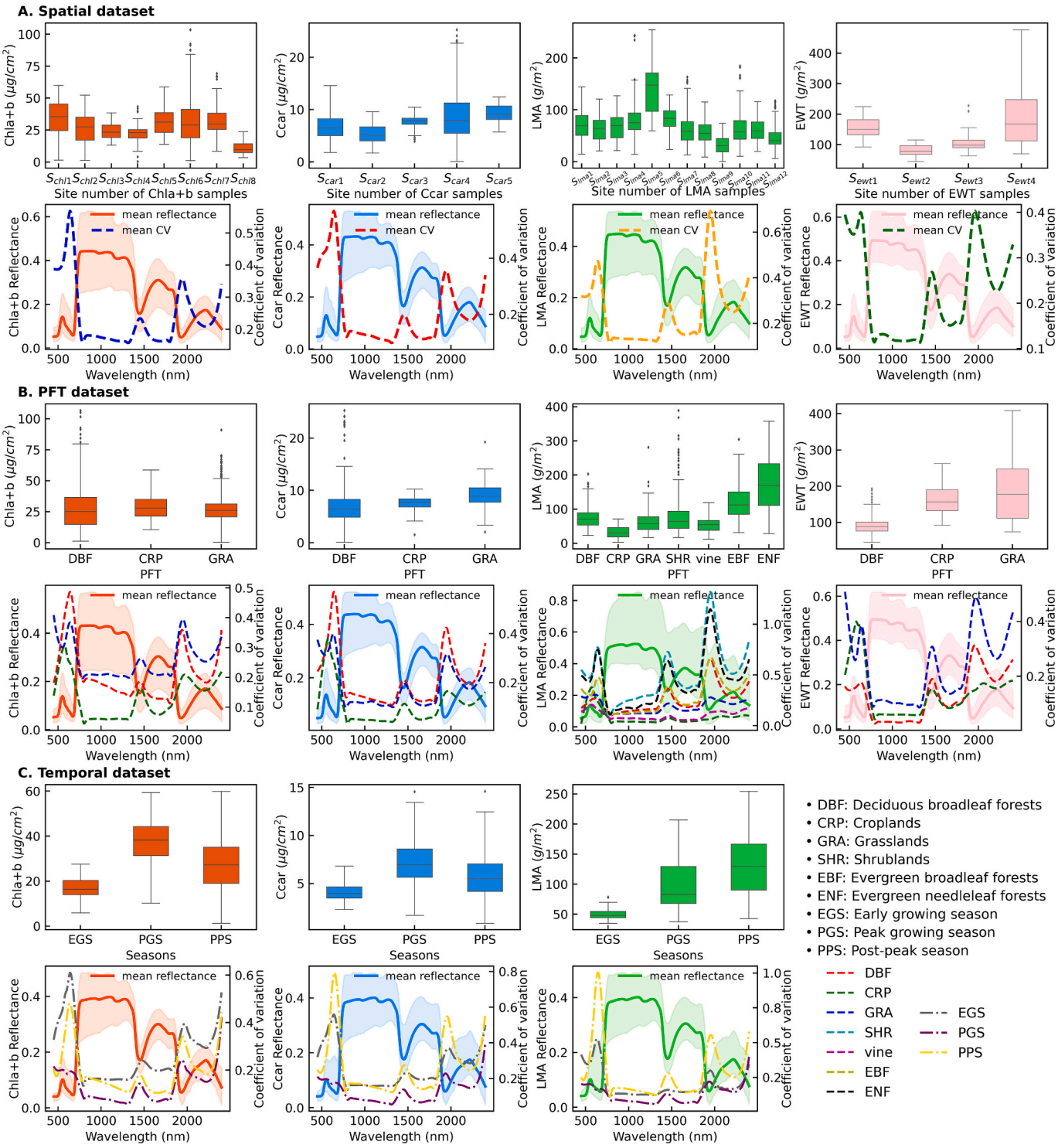

Fig. 3. Mean leaf traits, reflectance and variability (coefficient of variation, CV) among sites, plant functional types (PFTs) and growing season in the datasets. Panel A, B and C represent spatial, PFT and temporal dataset. The first row presents leaf traits across sites, PFTs and growing season; the second row represents the variability of leaf reflectance and CV across sites, PFTs and growing season. Each column corresponds to different leaf traits, Chla+b (chlorophyll contents), Ccar (carotenoid contents), LMA (leaf mass per area) and EWT (equivalent water thickness), respectively. The shaded areas refer to the standard deviation of reflectance.

1.4 %, 5.9 %, 1.0 %, 1.9 %, respectively. Similarly, for DNN models pretrained with Leaf-SIP simulated synthetic data, the R^2 values are 0.97 for Chla+b, 0.91 for Ccar, 0.99 for EWT, and 1.0 for LMA estimation, with *NRMSE* values of 4.6 %, 8.2 %, 2.9 %, and 0.6 %, respectively, with higher prediction errors observed for Ccar compared to other traits and PROSPECT model.

3.2.2. *Comparison of models' performance in predicting leaf traits*

Fig. 5 illustrates the averaged accuracy of different models to predict the four selected leaf traits (Chla+b, Ccar, EWT and LMA) using varying proportions of observations for model training or fine-tuning. The results show that the developed transfer learning models, TL(PROSPECT) and TL(Leaf-SIP), both consistently outperformed pure statistical models (GPR and PLSR) as well as RTMs (PROSPECT and Leaf-SIP). Specifically,

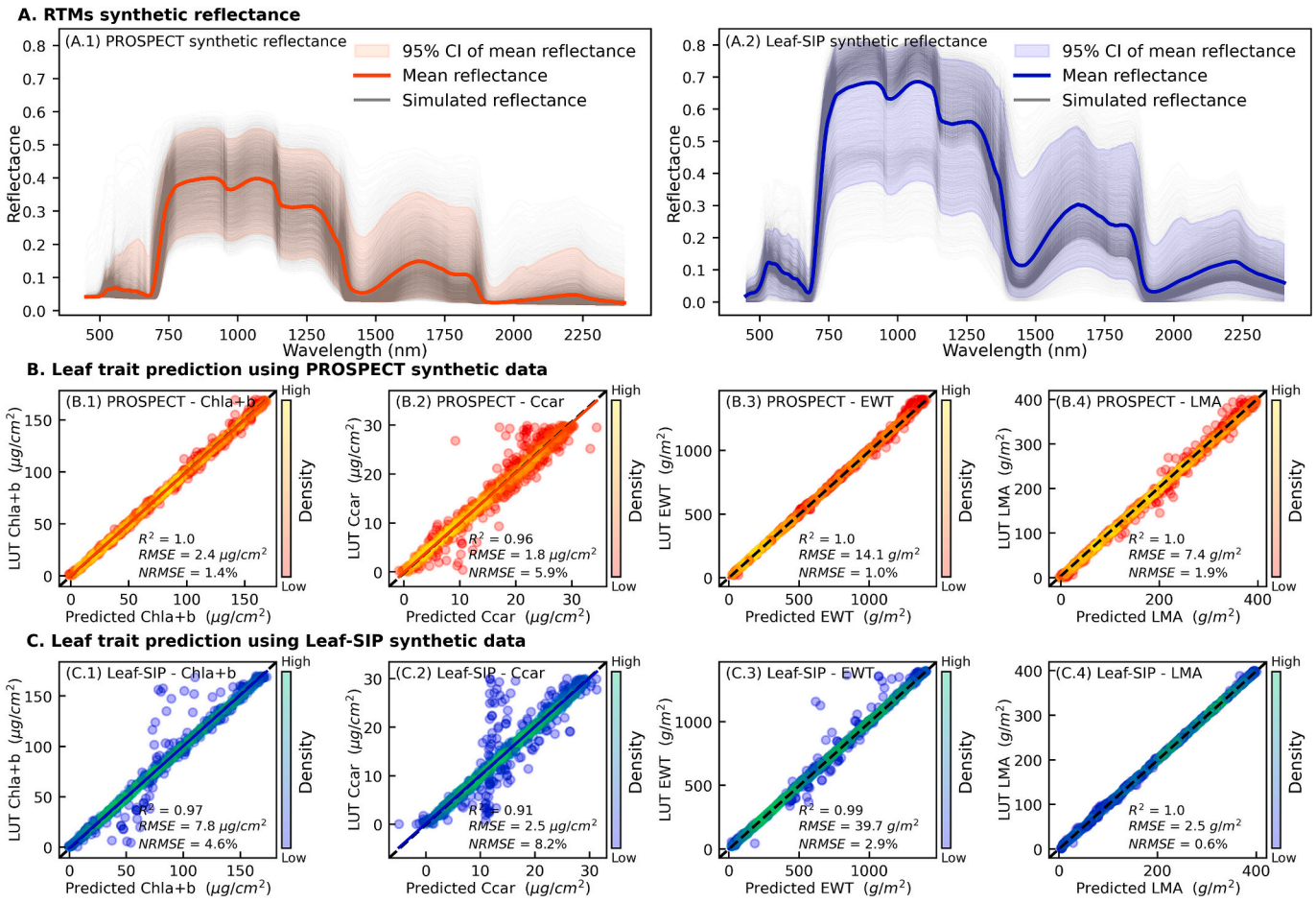

Fig. 4. Pre-training processes using the synthetic data of RTMs (PROSPECT and Leaf-SIP). A. RTMs synthetic reflectance; B. and C. The comparison of leaf trait prediction against their true values using pre-trained deep neural networks (DNN) models, which were trained by the paired leaf traits and simulated leaf reflectance generated from PROSPECT and Leaf-SIP, respectively.

TL (PROSPECT) models exhibited 0.08–0.17, 0.01–0.11, 0.45–0.79 and 0.4–0.64 higher R^2 and 1.63 % – 3.09 %, 0.06 % – 1.88 %, 10.7 % – 33.18 % and 9.89 % – 28.9 % lower *NRMSE* than GPR, PLSR, Pure Leaf-SIP and Pure PROSPECT, respectively. TL (Leaf-SIP) models exhibited 0.13–0.17, 0–0.1, 0.48–0.78 and 0.44–0.63 higher of R^2 and 1.67 % – 3.05 %, 0.09 % – 1.84 %, 10.74 % – 33.25 % and 9.99 % – 29.0 % lower of *NRMSE* than GPR, PLSR, Pure Leaf-SIP and Pure PROSPECT, respectively. The results of ANOVA test for the predictions of different models indicate significant differences between models ($p < 0.001$). Notably, the pure RTMs exhibited the poorest performance across all analyses, followed by GPR and PLSR models and the performance disparity was most pronounced when limited observations were incorporated for training or fine-tuning. However, as the size of the training or fine-tuning set increased, the rate of performance improvement diminished, although the differences are still large. Leading to reduced performance differences between different models.

Table S3 and Fig. S1-S8 present the accuracy statistics and corresponding scatter plots for each trait prediction. The performance of transfer learning models for each trait model prediction is always better as the size of the training or fine-tuning dataset increases. Specifically, for Chla+b and Ccar models, transfer learning models achieved R^2 values ranging from 0.6 ± 0.06 (mean ± 1SD, same in the following text) to 0.81 ± 0.07 and 0.5 ± 0.13 to 0.78 ± 0.1, respectively. These results surpass the performance of GPR models with R^2 values of 0.45 ± 0.05 to 0.63 ± 0.04 and 0.41 ± 0.03 to 0.58 ± 0.05, respectively, and PLSR models with R^2 values of 0.55 ± 0.06 to 0.72 ± 0.04 and 0.49 ± 0.05 to 0.66 ± 0.06, respectively. RTMs had even lower R^2 values of 0.17 to 0.3 and 0.01 to 0.06, respectively. Similarly, transfer learning models for predicting EWT achieved R^2 values spanning from 0.77 ± 0.07 to 0.95 ± 0.02. These results are comparable to those PLSR, which exhibited R^2 values from 0.86 ± 0.05 to 0.94 ± 0.02 and are higher than those of GPR models (0.66 ± 0.08 to 0.88 ± 0.04), RTMs (0.75 to 0.82). For LMA models, transfer learning models exhibited R^2 values from 0.68 ± 0.07 to 0.83 ± 0.05, outperforming the GPR models, which ranged from 0.6 ± 0.06 to 0.76 ± 0.06, the PLSR models with R^2 values from 0.7 ± 0.03 to 0.79 ± 0.05, RTMs with values of 0.08 to 0.11. Similar results were observed in *NRMSE* metric, indicating that transfer learning models provided better predictive accuracy than other models.

3.2.3. *Comparison of models' transferability in predicting leaf traits*

The strategies of "leave one site out," "leave one PFT out," and "leave one season out" were employed on the spatial, PFT, and temporal datasets, respectively to explore the transferability of the leaf trait estimation models. Notably, the transfer learning models exhibited the most robust performance outside their trained domains (Fig. 6, Table S4) in comparison to other state-of-the-art models. Specifically, the transfer learning models TL (PROSPECT) and TL (Leaf-SIP) exhibited mean R^2 values of 0.65, 0.57, 0.42 and 0.65, 0.56, 0.41, respectively, for spatial, PFT, and temporal transferability. Additionally, the *NRMSE* values were 18.26 %, 18.27 %, 23.66 % for TL (PROSPECT) and 18.82 %, 17.95 %, 22.3 % for TL (Leaf-SIP) across these categories. Transfer learning models outperformed GPR, which showed R^2 values of 0.6, 0.49, 0.36 and *NRMSE* values of 18.96 %, 18.35 %, 23.12 %; PLSR with R^2 values of 0.61, 0.46, 0.35 and *NRMSE* values of 20.99 %, 23.58 %, 28.27 %; Pure

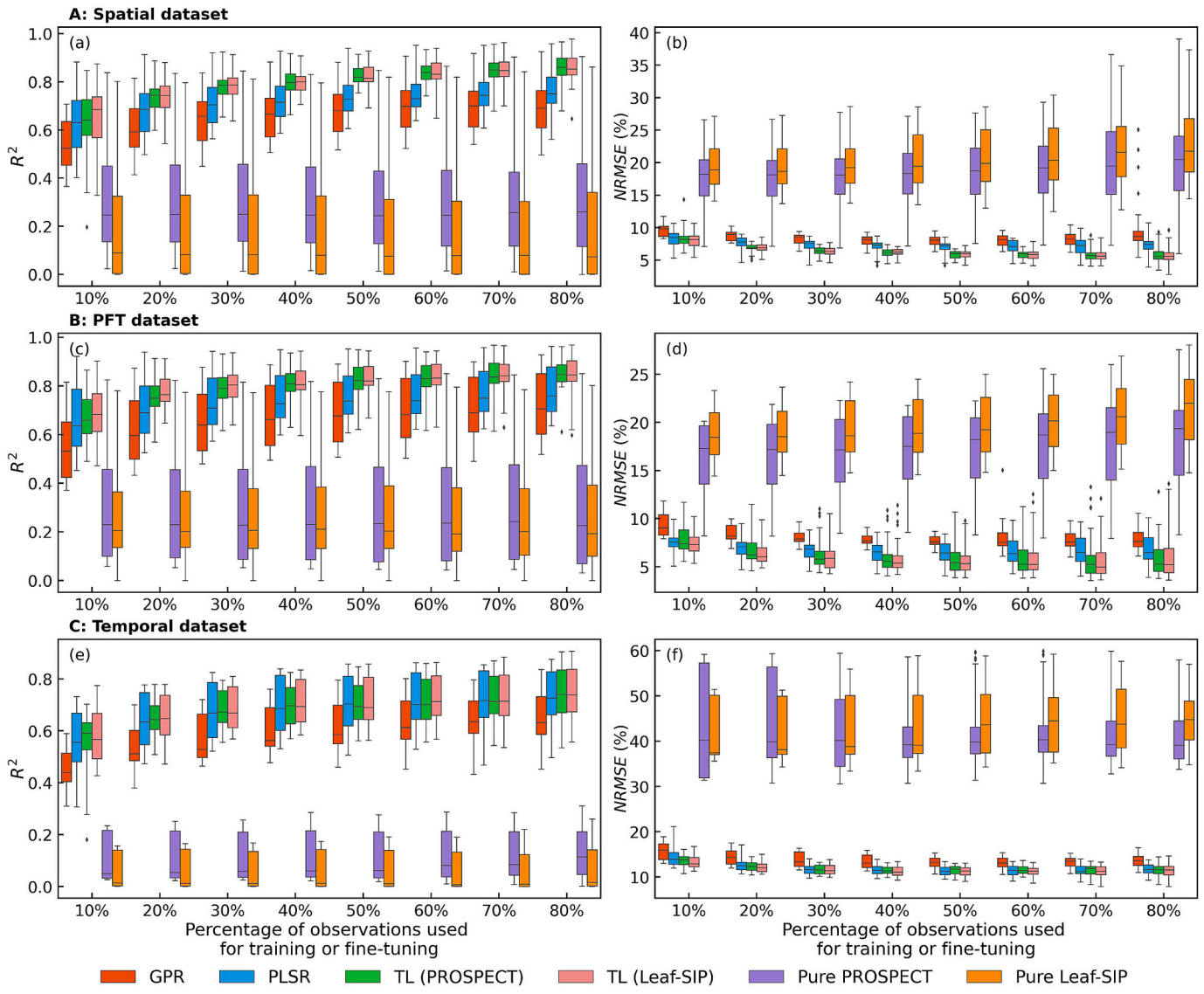

Fig. 5. The performance of different models in predicting leaf traits by incorporating varying proportions of observations for model training or fine-tuning. TL (PROSPECT) and TL(Leaf-SIP) refer to the transfer learning models developed by fine-tuning the pre-trained DNN models based on PROSPECT and Leaf-SIP synthetic data, respectively. Panel A. Spatial dataset; panel B. PFT dataset; panel C. Temporal dataset. (a), (c) and (e) refer to R^2 of leaf trait estimation in different datasets; (b), (d) and (f) refer to *NRMSE* of leaf trait estimation in different datasets.

PROSPECT with R^2 values of 0.6, 0.41, 0.12 and *NRMSE* values of 26.24 %, 20.9 %, 51.29 %; and Pure Leaf-SIP with R^2 values of 0.33, 0.28, 0.13 and *NRMSE* values of 25.07 %, 24.45 %, 53.11 %, for spatial, PFT, and temporal extrapolation, respectively. The ANOVA test results for the leaf trait predictions across out-of-trained domains of different models also revealed significant differences between the models ($p < 0.001$).

4. Discussion

In this study, we collected the leaf traits and leaf spectra observations across diverse sites, PFTs, and seasons using data from a previously compiled large dataset (Ji et al., 2024). Both leaf traits and leaf spectra exhibited significant variations across different sites, PFTs, and seasons ($p < 0.001$) (Fig. 4, Table S1). The variations are driven by the environmental heterogeneity (Albert et al., 2010; Jung, 2022; Messier et al., 2017; Messier et al., 2010), including differences in resource availability (e.g., nutrients and water), seasonal phenology, and functional adaptations across PFTs (Chavana-Bryant et al., 2017; Regos et al., 2022; Serbin et al., 2019; Stein and Kreft, 2015; Wu et al., 2017). Such factors highlight the interplay between biotic and abiotic influences in shaping leaf traits and spectral properties across ecosystems.

During the model pre-training process, differences in synthetic reflectance simulated by PROSPECT and Leaf-SIP (Fig. 4A) illustrate the impact of model structures on their outputs. Leaf-SIP generally predicts higher reflectance across wavelengths. However, this results in higher uncertainty for certain traits in the pre-trained DNN model, such as Ccar (Fig. 4C). Despite these differences, transfer learning models demonstrated broadly consistent performance across both RTMs. Nevertheless, our results suggest that the choice of RTM remains an important consideration, as discrepancies in model structures and assumptions can influence trait estimation accuracy. Thus, while TL methods can partially mitigate discrepancies arising from RTM choice, users should not dismiss careful RTM selection for pretraining. Overall, our results indicate the effectiveness of integrating leaf spectroscopy with both RTMs and statistical models for estimating leaf traits, while also emphasizing the importance of thoughtful RTM selection when applying transfer learning approaches. Statistical models, including GPR and PLSR, consistently outperformed the PROSPECT and Leaf-SIP RTMs

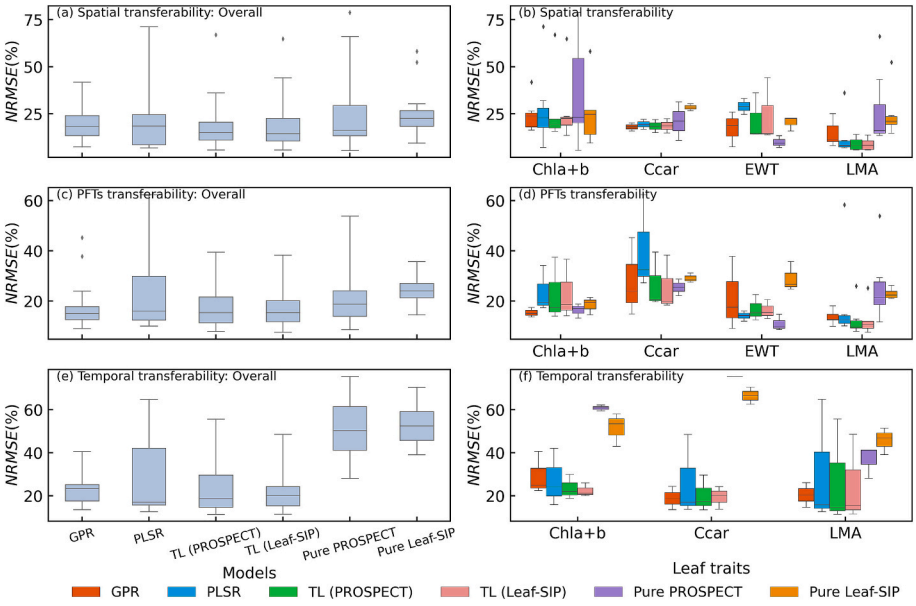

Fig. 6. Out-of-domains performance of different models. TL(PROSPECT) and TL(Leaf-SIP) refer to the transfer learning models developed by fine-tuning the pre-trained DNN models based on PROSPECT and Leaf-SIP synthetic data, respectively. (a), (c) and (e) refer to mean *NRMSE* of different models for predicting leaf traits out of spatial, PFT and temporal training domains; (b), (d) and (f) refer to *NRMSE* of different models for predicting leaf trait estimation out of spatial, PFT and temporal training domains.

(Fig. 5 and detailed in Table S3 and Fig. S1-S8). Notably, the statistical models demonstrated comparable performance in estimating Chla+b, Ccar, EWT, and LMA with previous studies (Chen et al., 2022; Cherif et al., 2023; Serbin et al., 2019; Xie et al., 2021). In the statistical models employed, PLSR exhibited higher accuracy than GPR, potentially due to GPR's sensitivity to hyperparameter tuning and challenges in dealing with high-dimensional hyperspectral data (Rivera-Caicedo et al., 2017). The superior performance of statistical models can be attributed to their ability to learn complex patterns and relationships from the available training data. In contrast, the RTMs show strong physical basis while they rely on the simplified assumptions and predefined physical interpretation of the interaction between electromagnetic radiation and leaf constituents (Feret et al., 2008; Jacquemoud et al., 1996; Jacquemoud and Baret, 1990; Wu et al., 2021), leading to limitations in representing intricate relationships present in real-world data, potentially due to the inherent constraints of the models themselves or suboptimal parameterization. As well, many RTM parameters, such as specific absorptivities, refractive index are actually empirically calibrated (Verrelst et al., 2019; Wang et al., 2021; Wang et al., 2015) using specific datasets like LOPEX (Hosgood et al., 1994) and ANGERS (Jacquemound et al., 2003), which may not fully capture the diversity of the internal leaf structure as well as pigment mixtures and absorption features in our compiled datasets (Peñuelas et al., 1993; Proctor and He, 2013; Villa et al., 2024). These factors collectively contribute to the overall poor predictive performance of both PROSPECT and Leaf-SIP models, particularly for leaf carotenoid pigments and LMA estimation. The poor predictability of carotenoids is attributed to overlapping absorption features with chlorophyll content. Similarly, the poor predictability of LMA is due to the overlapping absorption features with water and the use of a single specific absorption coefficient in RTMs to model its influence on optical properties (Ali et al., 2016; Colombo et al., 2008; Féret et al., 2019; Feret et al., 2008; Jacquemoud et al., 1996). Furthermore, the two RTMs, PROSPECT and Leaf-SIP, exhibited different accuracies, which highlights the uncertainties introduced by differences in model structures. These structural differences, such as variations in the treatment of light absorption, scattering, and internal leaf organization, can lead to divergent reflectance predictions and ultimately influence model performance in trait estimation tasks.

The proposed transfer learning models (TL(PROSPECT) and TL(Leaf-SIP)) for leaf traits estimation consistently outperformed pure statistical models (GPR, and PLSR) as well as RTMs (PROSPECT and Leaf-SIP) (Fig. 5, Table S3, Figs. S1-S8). This finding aligns with several previous studies (Wan et al., 2022; Wang et al., 2023a, 2023b; Zhang et al., 2021). The proposed transfer learning models incorporated domain knowledge from RTMs through synthetic data pre-training processes as well as acquired knowledge from real observational data utilized through fine-tuning processes. This dual-learning approach enhances model robustness, enabling it to adapt to variations in spectra and traits resulting from diverse and heterogeneous environmental conditions. Through fine-tuning processes, these models can mitigate uncertainties inherent in RTMs, which rely on simplified assumptions and predefined physical interpretations, leading to superior predictive performance. Moreover, the transfer learning models leverage synthetic data from RTMs for pre-training, requiring only limited labeled data for fine-tuning and yielding promising results. This reduces the dependency on large volumes of observational data necessary for pure statistical models. To further support this, we conducted an additional experiment on anthocyanin (Cant) prediction, Anthocyanin datasets are relatively rare in the research community, and for this study, we collected 192 Cant samples along with corresponding leaf spectra from previous studies (Gitelson et al., 2009; Gitelson et al., 2006; Merzlyak et al., 2008) The dataset includes three species: Siberian dogwood (*Cornus alba L.*), Norway maple (*Acer platanoides L.*) and Virginia creeper (*Parthenocissus quinquefolia (L.) Planch.*), respectively. Spectral measurements were acquired using a Hitachi 150–20 spectrophotometer (Tokyo, Japan) with an integrating sphere. Despite the limited sample size, the TL model consistently outperformed GPR and PLSR (Fig. S9). With only 10 % of the samples used for fine-tuning, the TL model achieved an R^2 of 0.62 and an NRMSE of 18.84 % (Fig. S9C.1), significantly outperforming GPR ($R^2 = 0.37$, NRMSE = 25.2 %) and PLSR ($R^2 = 0.2$, NRMSE = 60.2 %) (Fig. S9 A.1 and B.1). As the amount of fine-tuning data increased beyond 30 %, the TL model's performance improved further, reaching an R^2 above 0.8 and an NRMSE below 12.5 % (Fig. S9 C.2 – C.4). Furthermore, the transferability of the TL model was significantly better than that of GPR and PLSR. In the leave-one-PFT-out validation, the TL model maintained strong predictive performance across plant functional

types, whereas GPR and PLSR showed substantial declines in accuracy (Fig. S9A.5, B.5 and C.5). This analysis further underscores the advantage of TL models in handling scenarios with limited labeled data, demonstrating their effectiveness in improving leaf trait estimation while ensuring strong model generalization across diverse datasets.

The results, as indicated by out-of-domain accuracy (Fig. 6), demonstrated that the proposed transfer learning models are relatively more transferable than the statistical models. Our findings agree with the prior research that the statistical models are facing the challenges in maintaining stability and transferability across species (Helsen et al., 2021), across sites (Nakaji et al., 2019; Yan et al., 2021) and across phenological stages (Chlus and Townsend, 2022; Schiefer et al., 2021; Yang et al., 2016). This limitation is attributed to the inherent issue of statistical models where the variations in training data may not adequately represent or overlap with the variations in unseen data, leading to poor model performance when applied to novel datasets (Ji et al., 2024). Pure RTMs consistently exhibit the lowest performance within and outside their domains largely due to model simplifications and assumptions (Fig. 6). The transfer learning models, by incorporating domain knowledge from RTMs and fine-tuning with in-situ observations, ensure a balanced performance, transferability, and stability of the model (Wang et al., 2023b; Zhang et al., 2021).

Many studies have demonstrated that canopy spectra properties are capable of inferring leaf traits (Cherif et al., 2023; Estévez et al., 2021; Tagliabue et al., 2022; Verrelst et al., 2021; Wang et al., 2023b; Wang et al., 2021; Zhang et al., 2021). Built on this foundation, our proposed transfer learning models, initially developed at the leaf scale, offer significant potential for scalability to canopy scales by leveraging pre-training the canopy RTMs simulated synthetic data, such as PROSAIL (Jacquemoud et al., 2009). However, the effective implementation of these models at canopy scales requires careful consideration of factors like soil background, topography, illumination and viewing geometries as well as canopy structure, including leaf angle distribution, leaf area index, and clumping index. Addressing these complexities enhances the potential of transfer learning models to bridge the gap between leaf-scale measurements and large-scale remote sensing observations. Unlike purely data-driven models, our approach minimizes dependence on extensive in-situ calibration data, instead fine-tuning domain knowledge derived from RTMs. This enables accurate prediction of foliar traits across broader spatial scales.

Such capability is particularly relevant given the growing availability of current and upcoming global spaceborne hyperspectral missions such as ESA's CHIME (Nieke and Rast, 2018), NASA's EMIT (Green et al., 2020) and SBG (Cawse-Nicholson et al., 2021), which aim to monitor vegetation traits globally. These missions are unlikely to have globally comprehensive in-situ datasets for calibrating statistical models, making transfer learning a valuable tool for scaling trait estimation across diverse ecosystems. Statistical models demonstrate the capability to estimate various leaf traits when calibration data are accessible. However, RTMs remain limited to a specific subset of leaf traits, even as they continue to evolve, such as the inclusion of nitrogen in PROSPECT-PRO (Féret et al., 2021) and xanthophylls in Fluspect (Vilfan et al., 2018).

This limitation also extends to the proposed transfer learning models, which rely on domain knowledge from RTMs, restricting their application to traits such as Chla+b, Ccar, EWT, LMA, and certain pigments like brown pigments and anthocyanin pigments. Additionally, it is important to acknowledge that the temporal transferability test in this study was based on relatively unbalanced subsets across different phenological stages, which may have affected the robustness of the results for temporal transferability compared to transferability across PFTs and sites. Despite these limitations, the integration of RTM-based transfer learning with statistical approaches represents a promising avenue for advancing trait estimation across scales. By combining the strengths of physics-based models with the flexibility of machine learning, transfer learning models can bridge the gap between traditional RTMs and purely data-driven approaches. Future efforts should focus on expanding the range of RTMs to incorporate additional traits and refining transfer learning models to improve their scalability and applicability across diverse ecosystems. These advancements will be critical for leveraging emerging global hyperspectral datasets and addressing pressing ecological and environmental challenges.

Beyond model limitations, the inconsistencies in sampling protocols and measurement methods can introduce uncertainties in leaf optical measurements, potentially affecting the relationships between leaf spectra and traits. In our previous study (Ji et al., 2024), we have examined the effects of spectroradiometers on model transferability by selecting the measurements using ASD FieldSpec 3, PSR 3500+, and SVC HR-1024i that shared the identical location, PFT, and time. This analysis demonstrated promising model performance in cross-sensor validation, indicating minimal inconsistencies among spectroradiometers in terms of model transferability. Another key challenge when working with heterogeneous datasets is the influence of different spectral measurement setups. Many studies have utilized the leaf directional-hemispherical reflectance (DHRF) obtained from integrating spheres as input for RTMs in leaf trait prediction (Féret et al., 2019; Spafford et al., 2021). However, Z. Wang et al. (2023) has confirmed the capability of leaf bidirectional reflectance factor (BRF) — obtained using leaf clips or contact probes — for leaf trait estimation using RTMs. Their findings showed that BRF-based predictions achieved accuracy comparable to those using DHRF. Additionally, a simplified relationship between DHRF and BRF spectra has been established: $BRF(\lambda) = DHRF(\lambda) + b$, where λ represents wavelength and b is a wavelength-independent factor accounting for the difference in specular reflectance between BRF and DHRF spectra (Jay et al., 2016; Li et al., 2018, 2019). In this study, we investigated the effect of spectral measurement methods on model performance by categorizing samples into DHRF and BRF groups based on their measurement techniques. These grouped samples were then used as inputs for the trained transfer learning models. The results (Fig. S10) demonstrated high accuracy for both DHRF and BRF estimations, with R^2 values of 0.75, 0.60, 0.91, and 0.71 for Chl a + b, Ccar, EWT, and LMA, respectively, using DHRF. Similarly, the BRF-based estimations achieved R^2 values of 0.83, 0.86, 0.89, and 0.69, respectively. These results confirm that our transfer learning model is well-suited for both types of reflectance data.

5. Conclusions

Numerous models have been developed to predict leaf traits based on leaf spectroscopy, each of which has its limitations. The absence of universally high-performing, transferable, and stable models across different domains hinder our ability to quantify and comprehend spatiotemporal variations in leaf traits and their responses to environmental changes and biodiversity in terrestrial ecosystems. In this study, we ensembled three types of datasets, with significant variability in leaf traits and leaf spectra across different locations, PFTs, and seasons. Our proposed transfer learning models, incorporating domain knowledge from RTMs and limited observational data, achieved better predictive performance compared to other statistical models and pure RTMs. Most importantly, the transfer learning models exhibited higher transferability than statistical models. Our study underscores that transfer learning models can harness the advantages of both RTMs and statistical models and represent a promising approach for effectively predicting leaf traits.

CRediT authorship contribution statement

Fujiang Ji: Writing – review & editing, Writing – original draft, Visualization, Validation, Software, Resources, Methodology, Investigation, Formal analysis, Data curation, Conceptualization. **Fa Li:** Writing – review & editing, Methodology, Data curation, Conceptualization. **Hamid Dashti:** Writing – review & editing. **Dalei Hao:** Writing –

review & editing. **Philip A. Townsend:** Writing – review & editing. **Ting Zheng:** Writing – review & editing. **Hangkai You:** Writing – review & editing. **Min Chen:** Writing – review & editing, Methodology, Funding acquisition, Data curation, Conceptualization.

Declaration of competing interest

The authors declare that they have no known competing financial interests or personal relationships that could have appeared to influence the work reported in this paper.

Data availability

The original leaf traits and leaf spectra compiled dataset can be found in our previous study (Ji et al., 2024). The modeling code and the subset datasets used in this study is publicly available on GitHub (https://github.com/UW-GCRL/transfer_learning_models).

Acknowledgments

This study is supported by the National Aeronautics and Space Administration (NASA) through Remote Sensing Theory (80NSSC21K0568), Commercial Smallsat Data Scientific Analysis (CSDSA) (80NSSC24K0054) and Terrestrial Ecology programs (80NSSC21K1702). M.C. also acknowledges support from a McIntire–-Stennis grant (1027576) from the National Institute of Food and Agriculture (NIFA), United States Department of Agriculture (USDA). T.Z. was supported by the NASA Surface Biology and Geology (SBG) project through JPL award 1673139 to the University of Wisconsin and NSF ASCEND Biology Integration Institute (BII) award DBI 2021898. We acknowledge high-performance computing support from the UW-Madison Center for High Throughput Computing (CHTC) in the Department of Computer Sciences (Center for High Throughput Computing, 2006). The CHTC is supported by UW-Madison, the Advanced Computing Initiative, the Wisconsin Alumni Research Foundation, the Wisconsin Institutes for Discovery, and the National Science Foundation, and is an active member of the OSG Consortium, which is supported by the National Science Foundation and the U.S. Department of Energy's Office of Science.

Appendix A. Supplementary data

Supplementary data to this article can be found online at https://doi.org/10.1016/j.rse.2025.114818.

References

Adjorlolo, C., Mutanga, O., Cho, M.A., Ismail, R., 2013. Spectral resampling based on user-defined inter-band correlation filter: C3 and C4 grass species classification. Int. J. Appl. Earth Observ. Geoinform. 21, 535–544. https://doi.org/10.1016/J.JAG.2012.07.011.

Adler, P.B., Fajardo, A., Kleinhesselink, A.R., Kraft, N.J.B., 2013. Trait-based tests of coexistence mechanisms. Ecol. Lett. 16, 1294–1306. https://doi.org/10.1111/ELE.12157.

Albert, C.H., Thuiller, W., Yoccoz, N.G., Douzet, R., Aubert, S., Lavorel, S., 2010. A multi-trait approach reveals the structure and the relative importance of intra- vs. interspecific variability in plant traits. Funct. Ecol. 24, 1192–1201. https://doi.org/10.1111/J.1365-2435.2010.01727.X.

Ali, A.M., Darvishzadeh, R., Skidmore, A.K., van Duren, I., Heiden, U., Heurich, M., 2016. Estimating leaf functional traits by inversion of PROSPECT: assessing leaf dry matter content and specific leaf area in mixed mountainous forest. Int. J. Appl. Earth Observ. Geoinform. 45, 66–76. https://doi.org/10.1016/J.JAG.2015.11.004.

Allen, D.M., 1971. Mean square error of prediction as a criterion for selecting variables. Technometrics 13, 469–475. https://doi.org/10.1080/00401706.1971.10488811.

Allen, D.M., 1974. The relationship between variable selection and data Agumentation and a method for prediction. Technometrics 16, 125–127. https://doi.org/10.1080/00401706.1974.10489157.

Asner, G.P., Martin, R.E., 2008. Spectral and chemical analysis of tropical forests: scaling from leaf to canopy levels. Remote Sens. Environ. 112, 3958–3970. https://doi.org/10.1016/J.RSE.2008.07.003.

Asner, G.P., Martin, R.E., 2016. Spectranomics: emerging science and conservation opportunities at the interface of biodiversity and remote sensing. Glob Ecol. Conserv. 8, 212–219. https://doi.org/10.1016/J.GECCO.2016.09.010.

Berger, K., Atzberger, C., Danner, M., D'Urso, G., Mauser, W., Vuolo, F., Hank, T., 2018. Evaluation of the PROSAIL model capabilities for future hyperspectral model environments: a review study. Remote Sens. 10, 85. https://doi.org/10.3390/RS10010085.

Berger, K., Verrelst, J., Féret, J.B., Hank, T., Wocher, M., Mauser, W., Camps-Valls, G., 2020. Retrieval of aboveground crop nitrogen content with a hybrid machine learning method. Int. J. Appl. Earth Observ. Geoinform. 92, 102174. https://doi.org/10.1016/J.JAG.2020.102174.

Bergstra, J., Ca, J.B., Ca, Y.B., 2012. Random search for hyper-parameter optimization. J. Mach. Learn. Res. 13, 281–305. https://doi.org/10.5555/2188385.2188395.

Burnett, A.C., Serbin, S.P., Lamour, J., Anderson, J., Davidson, K.J., Yang, D., Rogers, A., 2021. Seasonal trends in photosynthesis and leaf traits in scarlet oak. Tree Physiol 41, 1413–1424. https://doi.org/10.1093/TREEPHYS/TPAB015.

Cawse-Nicholson, K., Townsend, P.A., Schimel, D., Assiri, A.M., Blake, P.L., Buongiorno, M.F., Campbell, P., Zhang, Q., et al., 2021. NASA'S surface biology and geology designated observable: a perspective on surface imaging algorithms. Remote Sens. Environ. 257, 112349. https://doi.org/10.1016/J.RSE.2021.112349.

Center for High Throughput Computing, 2006. Center for High Throughput Computing.

Chavana-Bryant, C., Malhi, Y., Wu, J., Asner, G.P., Anastasiou, A., Enquist, B.J., Cosio Caravasi, E.G., Doughty, C.E., Saleska, S.R., Martin, R.E., Gerard, F.F., 2017. Leaf aging of Amazonian canopy trees as revealed by spectral and physiochemical measurements. New Phytol. 214, 1049–1063. https://doi.org/10.1111/NPH.13853.

Chen, L., Zhang, Y., Nunes, M.H., Stoddart, J., Khoury, S., Chan, A.H.Y., Coomes, D.A., 2022. Predicting leaf traits of temperate broadleaf deciduous trees from hyperspectral reflectance: can a general model be applied across a growing season? Remote Sens. Environ. 269, 112767. https://doi.org/10.1016/J.RSE.2021.112767.

Cherif, E., Feilhauer, H., Berger, K., Dao, P.D., Ewald, M., Hank, T.B., He, Y., Kovach, K. R., Lu, B., Townsend, P.A., Kattenborn, T., 2023. From spectra to plant functional traits: transferable multi-trait models from heterogeneous and sparse data. Remote Sens. Environ. 292, 113580. https://doi.org/10.1016/J.RSE.2023.113580.

Chlus, A., Townsend, P.A., 2022. Characterizing seasonal variation in foliar biochemistry with airborne imaging spectroscopy. Remote Sens. Environ. 275, 113023. https://doi.org/10.1016/J.RSE.2022.113023.

Collins, C.G., Wright, S.J., Wurzburger, N., 2016. Root and leaf traits reflect distinct resource acquisition strategies in tropical lianas and trees. Oecologia 180, 1037–1047. https://doi.org/10.1007/S00442-015-3410-7/FIGURES/3.

Colombo, R., Meroni, M., Marchesi, A., Busetto, L., Rossini, M., Giardino, C., Panigada, C., 2008. Estimation of leaf and canopy water content in poplar plantations by means of hyperspectral indices and inverse modeling. Remote Sens. Environ. 112, 1820–1834. https://doi.org/10.1016/J.RSE.2007.09.005.

Combal, B., Baret, F., Weiss, M., Trubuil, A., Macé, D., Pragnère, A., Myneni, R., Knyazikhin, Y., Wang, L., 2003. Retrieval of canopy biophysical variables from bidirectional reflectance: using prior information to solve the ill-posed inverse problem. Remote Sens. Environ. 84, 1–15. https://doi.org/10.1016/S0034-4257(02)00035-4.

Cornwell, W.K., Pearse, W.D., Dalrymple, R.L., Zanne, A.E., 2019. What we (don't) know about global plant diversity. Ecography 42, 1819–1831. https://doi.org/10.1111/ecog.04481.

Dechant, B., Cuntz, M., Vohland, M., Schulz, E., Doktor, D., 2017. Estimation of photosynthesis traits from leaf reflectance spectra: correlation to nitrogen content as the dominant mechanism. Remote Sens. Environ. 196, 279–292. https://doi.org/10.1016/J.RSE.2017.05.019.

Dechant, B., Kattge, J., Pavlick, R., Schneider, F.D., Sabatini, F.M., Moreno-Martínez, Á., Butler, E.E., van Bodegom, P.M., Vallicrosa, H., Kattenborn, T., Boonman, C.C.F., Madani, N., Wright, I.J., Dong, N., Feilhauer, H., Peñuelas, J., Sardans, J., Aguirre-Gutiérrez, J., Reich, P.B., Leitão, P.J., Cavender-Bares, J., Myers-Smith, I.H., Durán, S.M., Croft, H., Prentice, I.C., Huth, A., Rebel, K., Zaehle, S., Šímová, I., Díaz, S., Reichstein, M., Schiller, C., Bruelheide, H., Mahecha, M., Wirth, C., Malhi, Y., Townsend, P.A., 2024. Intercomparison of global foliar trait maps reveals fundamental differences and limitations of upscaling approaches. Remote Sens. Environ. 311, 114276. https://doi.org/10.1016/J.RSE.2024.114276.

Doktor, D., Lausch, A., Spengler, D., Thurner, M., 2014. Extraction of plant physiological status from hyperspectral signatures using machine learning methods. Remote Sensing 6, 12247. https://doi.org/10.3390/RS61212247.

Estévez, J., Berger, K., Vicent, J., Rivera-Caicedo, J.P., Wocher, M., Verrelst, J., 2021. Top-of-atmosphere retrieval of multiple crop traits using Variational heteroscedastic Gaussian processes within a hybrid workflow. Remote Sensing 13, 1589. https://doi.org/10.3390/RS13081589.

Fajardo, A., Siefert, A., 2016. Phenological variation of leaf functional traits within species. Oecologia 180, 951–959. https://doi.org/10.1007/S00442-016-3545-1/FIGURES/3.

Fatichi, S., Pappas, C., Zscheischler, J., Leuzinger, S., 2019. Modelling carbon sources and sinks in terrestrial vegetation. New Phytol. 221, 652–668. https://doi.org/10.1111/NPH.15451.

Feret, J.B., François, C., Asner, G.P., Gitelson, A.A., Martin, R.E., Bidel, L.P.R., Ustin, S.L., le Maire, G., Jacquemoud, S., 2008. PROSPECT-4 and 5: advances in the leaf optical properties model separating photosynthetic pigments. Remote Sens. Environ. 112, 3030–3043. https://doi.org/10.1016/J.RSE.2008.02.012.

Féret, J.B., Gitelson, A.A., Noble, S.D., Jacquemoud, S., 2017. PROSPECT-D: towards modeling leaf optical properties through a complete lifecycle. Remote Sens. Environ. 193, 204–215. https://doi.org/10.1016/J.RSE.2017.03.004.

Féret, J.B., le Maire, G., Jay, S., Berveiller, D., Bendoula, R., Hmimina, G., Cheraiet, A., Oliveira, J.C., Ponzoni, F.J., Solanki, T., de Boissieu, F., Chave, J., Nouvellon, Y.,

Porcar-Castell, A., Proisy, C., Soudani, K., Gastellu-Etchegorry, J.P., Lefèvre-Fonollosa, M.J., 2019. Estimating leaf mass per area and equivalent water thickness based on leaf optical properties: potential and limitations of physical modeling and machine learning. Remote Sens. Environ. 231, 110959. https://doi.org/10.1016/J.RSE.2018.11.002.

Féret, J.B., Berger, K., de Boissieu, F., Malenovský, Z., 2021. PROSPECT-PRO for estimating content of nitrogen-containing leaf proteins and other carbon-based constituents. Remote Sens. Environ. 252, 112173. https://doi.org/10.1016/J.RSE.2020.112173.

Fu, P., Meacham-Hensold, K., Guan, K., Wu, J., Bernacchi, C., 2020. Estimating photosynthetic traits from reflectance spectra: a synthesis of spectral indices, numerical inversion, and partial least square regression. Plant Cell Environ. 43, 1241–1258. https://doi.org/10.1111/PCE.13718.

Gitelson, A.A., Keydan, G.P., Merzlyak, M.N., 2006. Three-band model for noninvasive estimation of chlorophyll, carotenoids, and anthocyanin contents in higher plant leaves. Geophys. Res. Lett. 33. https://doi.org/10.1029/2006GL026457.

Gitelson, A.A., Chivkunova, O.B., Merzlyak, M.N., 2009. Nondestructive estimation of anthocyanins and chlorophylls in anthocyanic leaves. Am. J. Bot. 96, 1861–1868. https://doi.org/10.3732/AJB.0800395.

Green, R.O., Mahowald, N., Ung, C., Thompson, D.R., Bator, L., Bennet, M., Bernas, M., Zan, J., et al., 2020. The earth surface mineral dust source investigation: an earth science imaging spectroscopy Mission. IEEE Aerospace Conf. Proc. https://doi.org/10.1109/AERO47225.2020.9172731.

Helsen, K., Bassi, L., Feilhauer, H., Kattenborn, T., Matsushima, H., Van Cleemput, E., Somers, B., Honnay, O., 2021. Evaluating different methods for retrieving intraspecific leaf trait variation from hyperspectral leaf reflectance. Ecol. Indic. 130, 108111. https://doi.org/10.1016/J.ECOLIND.2021.108111.

Herman, J., Usher, W., 2017. SALib: an open-source Python library for sensitivity analysis. J. Open Source Softw. 2, 97. https://doi.org/10.21105/JOSS.00097.

Hill, J., Buddenbaum, H., Townsend, P.A., 2019. Imaging spectroscopy of Forest ecosystems: perspectives for the use of space-borne hyperspectral earth observation systems. Surv. Geophys. 40, 553–588. https://doi.org/10.1007/S10712-019-09514-2/FIGURES/1.

Hornik, K., Stinchcombe, M., White, H., 1989. Multilayer feedforward networks are universal approximators. Neural Netw. 2, 359–366. https://doi.org/10.1016/0893-6080(89)90020-8.

Hosgood, B., Jacquemoud, S., Andreoli, G., Verdebout, J., Pedrini, G., Schmuck, G., 1994. Leaf Optical properties EXperiment 93 (LOPEX93). In: European Commission, Joint Research Centre, Institute for Remote Sensing Applications. Report EUR 16095 EN 11.

Ito, A., Muraoka, H., Koizumi, H., Saigusa, N., Murayama, S., Yamamoto, S., 2006. Seasonal variation in leaf properties and ecosystem carbon budget in a cool-temperate deciduous broad-leaved forest: simulation analysis at Takayama site, Japan. Ecol. Res. 21, 137–149. https://doi.org/10.1007/S11284-005-0100-7/FIGURES/6.

Jacquemoud, S., Baret, F., 1990. PROSPECT: a model of leaf optical properties spectra. Remote Sens. Environ. 34, 75–91. https://doi.org/10.1016/0034-4257(90)90100-Z.

Jacquemoud, S., Ustin, S.L., Verdebout, J., Schmuck, G., Andreoli, G., Hosgood, B., 1996. Estimating leaf biochemistry using the PROSPECT leaf optical properties model. Remote Sens. Environ. 56, 194–202. https://doi.org/10.1016/0034-4257(95)00238-3.

Jacquemoud, S., Verhoef, W., Baret, F., Bacour, C., Zarco-Tejada, P.J., Asner, G.P., François, C., Ustin, S.L., 2009. PROSPECT + SAIL models: a review of use for vegetation characterization. Remote Sens. Environ. 113, S56–S66. https://doi.org/10.1016/J.RSE.2008.01.026.

Jacquemound, S., Bidel, L., Francois, C., Pavan, G., 2003. ANGERS Leaf Optical properties database (2003). Data Set. Available online: http://ecosis. org (accessed on 5 June 2018).

Jay, S., Bendoula, R., Hadoux, X., Féret, J.B., Gorretta, N., 2016. A physically-based model for retrieving foliar biochemistry and leaf orientation using close-range imaging spectroscopy. Remote Sens. Environ. 177, 220–236. https://doi.org/10.1016/J.RSE.2016.02.029.

Ji, F., Li, F., Hao, D., Shiklomanov, A.N., Yang, X., Townsend, P.A., Dashti, H., Nakaji, T., Kovach, K.R., Liu, H., Luo, M., Chen, M., 2024. Unveiling the transferability of PLSR models for leaf trait estimation: lessons from a comprehensive analysis with a novel global dataset. New Phytol. 243, 111–131. https://doi.org/10.1111/NPH.19807.

Jiang, J., Comar, A., Weiss, M., Baret, F., 2021. FASPECT: a model of leaf optical properties accounting for the differences between upper and lower faces. Remote Sens. Environ. 253, 112205. https://doi.org/10.1016/J.RSE.2020.112205.

Jung, M., 2022. Predictability and transferability of local biodiversity environment relationships. PeerJ 10, e13872. https://doi.org/10.7717/PEERJ.13872.

Kattge, J., Bönisch, G., Díaz, S., Lavorel, S., Prentice, I.C., Leadley, P., Tautenhahn, S., Wirth, C., et al., 2020. TRY plant trait database – enhanced coverage and open access. Glob. Chang. Biol. 26, 119–188. https://doi.org/10.1111/GCB.14904.

Knyazikhin, Y., Martonchik, J.V., Myneni, R.B., Diner, D.J., Running, S.W., 1998. Synergistic algorithm for estimating vegetation canopy leaf area index and fraction of absorbed photosynthetically active radiation from MODIS and MISR data. J. Geophys. Res. Atmos. 103, 32257–32275. https://doi.org/10.1029/98JD02462.

Lewis, P., Disney, M., 2007. Spectral invariants and scattering across multiple scales from within-leaf to canopy. Remote Sens. Environ. 109, 196–206. https://doi.org/10.1016/J.RSE.2006.12.015.

Li, D., Cheng, T., Jia, M., Zhou, K., Lu, N., Yao, X., Tian, Y., Zhu, Y., Cao, W., 2018. PROCWT: coupling PROSPECT with continuous wavelet transform to improve the retrieval of foliar chemistry from leaf bidirectional reflectance spectra. Remote Sens. Environ. 206, 1–14. https://doi.org/10.1016/J.RSE.2017.12.013.

Li, D., Tian, L., Wan, Z., Jia, M., Yao, X., Tian, Y., Zhu, Y., Cao, W., Cheng, T., 2019. Assessment of unified models for estimating leaf chlorophyll content across directional-hemispherical reflectance and bidirectional reflectance spectra. Remote Sens. Environ. 231, 111240. https://doi.org/10.1016/J.RSE.2019.111240.

de Lima, R.P., Marfurt, K., 2019. Convolutional neural network for remote-sensing scene classification: transfer learning analysis. Remote Sensing 12, 86. https://doi.org/10.3390/RS12010086.

Ma, Y., Chen, S., Ermon, S., Lobell, D.B., 2024. Transfer learning in environmental remote sensing. Remote Sens. Environ. 301, 113924. https://doi.org/10.1016/J.RSE.2023.113924.

McKown, A.D., Guy, R.D., Azam, M.S., Drewes, E.C., Quamme, L.K., 2013. Seasonality and phenology alter functional leaf traits. Oecologia 172, 653–665. https://doi.org/10.1007/S00442-012-2531-5/TABLES/4.

Merzlyak, M.N., Chivkunova, O.B., Solovchenko, A.E., Naqvi, K.R., 2008. Light absorption by anthocyanins in juvenile, stressed, and senescing leaves. J. Exp. Bot. 59, 3903–3911. https://doi.org/10.1093/JXB/ERN230.

Messier, J., McGill, B.J., Lechowicz, M.J., 2010. How do traits vary across ecological scales? A case for trait-based ecology. Ecol. Lett. 13, 838–848. https://doi.org/10.1111/J.1461-0248.2010.01476.X.

Messier, J., McGill, B.J., Enquist, B.J., Lechowicz, M.J., 2017. Trait variation and integration across scales: is the leaf economic spectrum present at local scales? Ecography 40, 685–697. https://doi.org/10.1111/ECOG.02006.

Nakaji, T., Oguma, H., Nakamura, M., Kachina, P., Asanok, L., Marod, D., Aiba, M., Kurokawa, H., Kosugi, Y., Kassim, A.R., Hiura, T., 2019. Estimation of six leaf traits of east Asian forest tree species by leaf spectroscopy and partial least square regression. Remote Sens. Environ. 233, 111381. https://doi.org/10.1016/J.RSE.2019.111381.

Nieke, J., Rast, M., 2018. Towards the copernicus hyperspectral imaging mission for the environment (CHIME). In: International Geoscience and Remote Sensing Symposium (IGARSS) 2018-July, 157–159. https://doi.org/10.1109/IGARSS.2018.8518384.

Nowakowski, A., Mrziglod, J., Spiller, D., Bonifacio, R., Ferrari, I., Mathieu, P.P., Garcia-Herranz, M., Kim, D.H., 2021. Crop type mapping by using transfer learning. Int. J. Appl. Earth Observ. Geoinform. 98, 102313. https://doi.org/10.1016/J.JAG.2021.102313.

Peñuelas, J., Gamon, J.A., Griffin, K.L., Field, C.B., 1993. Assessing community type, plant biomass, pigment composition, and photosynthetic efficiency of aquatic vegetation from spectral reflectance. Remote Sens. Environ. 46, 110–118. https://doi.org/10.1016/0034-4257(93)90088-F.

Proctor, C., He, Y., 2013. Estimation of foliar pigment concentration in floating macrophytes using hyperspectral vegetation indices. Int. J. Remote Sens. 34, 8011–8027. https://doi.org/10.1080/01431161.2013.828183.

Rasmussen, C.E., 2004. Gaussian processes in machine learning. Lecture Notes in Computer Science (including subseries Lecture Notes in Artificial Intelligence and Lecture Notes in Bioinformatics) 3176, 63–71. https://doi.org/10.1007/978-3-540-28650-9_4/COVER.

Regos, A., Gonçalves, J., Arenas-Castro, S., Alcaraz-Segura, D., Guisan, A., Honrado, J.P., 2022. Mainstreaming remotely sensed ecosystem functioning in ecological niche models. Remote Sens. Ecol. Conserv. 8, 431–447. https://doi.org/10.1002/RSE2.255.

Reichstein, M., Bahn, M., Mahecha, M.D., Kattge, J., Baldocchi, D.D., 2014. Linking plant and ecosystem functional biogeography. Proc. Natl. Acad. Sci. U. S. A. 111, 13697–13702. https://doi.org/10.1073/PNAS.1216065111/SUPPL_FILE/PNAS.1216065111.SAPP.PDF.

Reichstein, M., Camps-Valls, G., Stevens, B., Jung, M., Denzler, J., Carvalhais, N., Prabhat, 2019. Deep learning and process understanding for data-driven Earth system science. Nature 566, 195–204. https://doi.org/10.1038/s41586-019-0912-1.

Rivera-Caicedo, J.P., Verrelst, J., Muñoz-Marí, J., Camps-Valls, G., Moreno, J., 2017. Hyperspectral dimensionality reduction for biophysical variable statistical retrieval. ISPRS J. Photogramm. Remote Sens. 132, 88–101. https://doi.org/10.1016/J.ISPRSJPRS.2017.08.012.

Rogers, A., Medlyn, B.E., Dukes, J.S., Bonan, G., von Caemmerer, S., Dietze, M.C., Kattge, J., Leakey, A.D.B., Mercado, L.M., Niinemets, Ü., Prentice, I.C., Serbin, S.P., Sitch, S., Way, D.A., Zaehle, S., 2017. A roadmap for improving the representation of photosynthesis in earth system models. New Phytol. 213, 22–42. https://doi.org/10.1111/NPH.14283.

Schiefer, F., Schmidtlein, S., Kattenborn, T., 2021. The retrieval of plant functional traits from canopy spectra through RTM-inversions and statistical models are both critically affected by plant phenology. Ecol. Indic. 121, 107062. https://doi.org/10.1016/J.ECOLIND.2020.107062.

Schimel, D., Schneider, F.D., Carbon, J., Participants, E., 2019. Flux towers in the sky: global ecology from space. New Phytol. 224, 570–584. https://doi.org/10.1111/NPH.15934.

Schlemmera, M., Gitelson, A., Schepersa, J., Fergusona, R., Peng, Y., Shanahana, J., Rundquist, D., 2013. Remote estimation of nitrogen and chlorophyll contents in maize at leaf and canopy levels. Int. J. Appl. Earth Obs. Geoinf. 25, 47–54. https://doi.org/10.1016/J.JAG.2013.04.003.

Serbin, S.P., Wu, J., Ely, K.S., Kruger, E.L., Townsend, P.A., Meng, R., Wolfe, B.T., Chlus, A., Wang, Z., Rogers, A., 2019. From the Arctic to the tropics: multibiome prediction of leaf mass per area using leaf reflectance. New Phytol. 224, 1557–1568. https://doi.org/10.1111/NPH.16123.

Shabani, A., Ghaffary, K.A., Sepaskhah, A.R., Kamgar-Haghighi, A.A., 2017. Using the artificial neural network to estimate leaf area. Sci. Hortic. 216, 103–110. https://doi.org/10.1016/J.SCIENTA.2016.12.032.

Shen, Z., Ramirez-Lopez, L., Behrens, T., Cui, L., Zhang, M., Walden, L., Wetterlind, J., Shi, Z., Sudduth, K.A., Baumann, P., Song, Y., Catambay, K., Viscarra Rossel, R.A., 2022. Deep transfer learning of global spectra for local soil carbon monitoring. ISPRS

J. Photogramm. Remote Sens. 188, 190–200. https://doi.org/10.1016/J.ISPRSJPRS.2022.04.009.
Skidmore, A.K., Coops, N.C., Neinavaz, E., Ali, A., Schaepman, M.E., Paganini, M., Kissling, W.D., Vihervaara, P., Darvishzadeh, R., Feilhauer, H., Fernandez, M., Fernández, N., Gorelick, N., Geijzendorffer, I., Heiden, U., Heurich, M., Hobern, D., Holzwarth, S., Muller-Karger, F.E., Van De Kerchove, R., Lausch, A., Leitão, P.J., Lock, M.C., Mücher, C.A., O'Connor, B., Rocchini, D., Turner, W., Vis, J.K., Wang, T., Wegmann, M., Wingate, V., 2021. Priority list of biodiversity metrics to observe from space. Nat. Ecol. Evol. 5, 896–906. https://doi.org/10.1038/s41559-021-01451-x.
Spafford, L., le Maire, G., MacDougall, A., de Boissieu, F., Féret, J.B., 2021. Spectral subdomains and prior estimation of leaf structure improves PROSPECT inversion on reflectance or transmittance alone. Remote Sens. Environ. 252, 112176. https://doi.org/10.1016/J.RSE.2020.112176.
Stein, A., Kreft, H., 2015. Terminology and quantification of environmental heterogeneity in species-richness research. Biol. Rev. 90, 815–836. https://doi.org/10.1111/BRV.12135.
Stenberg, P., Mõttus, M., Rautiainen, M., 2016. Photon recollision probability in modelling the radiation regime of canopies — a review. Remote Sens. Environ. 183, 98–108. https://doi.org/10.1016/J.RSE.2016.05.013.
Storn, R., Price, K., 1997. Differential evolution – a simple and efficient heuristic for global optimization over continuous spaces. J. Glob. Optim. 11, 341–359. https://doi.org/10.1023/A:1008202821328.
Szollosi, E., Oláh, V., Kanalas, P., Kis, J., Fenyvesi, A., Mészáros, I., 2011. Seasonal variation of leaf ecophysiological traits within the canopy of Quercus petraea (Matt.) Liebl. trees. Acta Biol Hung 61, 172–188. https://doi.org/10.1556/ABIOL.61.2010.SUPPL.17.
Tagliabue, G., Boschetti, M., Bramati, G., Candiani, G., Colombo, R., Nutini, F., Pompilio, L., Rivera-Caicedo, J.P., Rossi, M., Rossini, M., Verrelst, J., Panigada, C., 2022. Hybrid retrieval of crop traits from multi-temporal PRISMA hyperspectral imagery. ISPRS J. Photogram. Rem. Sens. 187, 362–377. https://doi.org/10.1016/J.ISPRSJPRS.2022.03.014.
Townsend, P.A., Foster, J.R., Chastain, R.A., Currie, W.S., 2003. Application of imaging spectroscopy to mapping canopy nitrogen in the forest of the central Appalachian mountains using hyperion and AVIRIS. IEEE Trans. Geosci. Remote Sens. 41, 1347–1354. https://doi.org/10.1109/TGRS.2003.813205.
Van Bodegom, P.M., Douma, J.C., Verheijen, L.M., 2014. A fully traits-based approach to modeling global vegetation distribution. Proc. Natl. Acad. Sci. U. S. A. 111, 13733–13738. https://doi.org/10.1073/PNAS.1304551110/SUPPL_FILE/PNAS.1304551110.SAPP.PDF.
Vendramini, F., Díaz, S., Gurvich, D.E., Wilson, P.J., Thompson, K., Hodgson, J.G., 2002. Leaf traits as indicators of resource-use strategy in floras with succulent species. New Phytol. 154, 147–157. https://doi.org/10.1046/J.1469-8137.2002.00357.X.
Verger, A., Baret, F., Camacho, F., 2011. Optimal modalities for radiative transfer-neural network estimation of canopy biophysical characteristics: evaluation over an agricultural area with CHRIS/PROBA observations. Remote Sens. Environ. 115, 415–426. https://doi.org/10.1016/J.RSE.2010.09.012.
Verrelst, J., Malenovský, Z., Van der Tol, C., Camps-Valls, G., Gastellu-Etchegorry, J.P., Lewis, P., North, P., Moreno, J., 2019. Quantifying vegetation biophysical variables from imaging spectroscopy data: a review on retrieval methods. Surv. Geophys. 40, 589–629. https://doi.org/10.1007/S10712-018-9478-Y/FIGURES/9.
Verrelst, J., Berger, K., Rivera-Caicedo, J.P., 2021. Intelligent sampling for vegetation nitrogen mapping based on hybrid machine learning algorithms. IEEE Geosci. Remote Sens. Lett. 18, 2038–2042. https://doi.org/10.1109/LGRS.2020.3014676.
Vilfan, N., Van der Tol, C., Yang, P., Wyber, R., Malenovský, Z., Robinson, S.A., Verhoef, W., 2018. Extending Fluspect to simulate xanthophyll driven leaf reflectance dynamics. Remote Sens. Environ. 211, 345–356. https://doi.org/10.1016/J.RSE.2018.04.012.
Villa, P., Dalla Vecchia, A., Piaser, E., Bolpagni, R., 2024. Assessing PROSPECT performance on aquatic plant leaves. Remote Sens. Environ. 301, 113926. https://doi.org/10.1016/J.RSE.2023.113926.
Wan, L., Zhang, J., Xu, Y., Huang, Y., Zhou, W., Jiang, L., He, Y., Cen, H., 2021. PROSDM: applicability of PROSPECT model coupled with spectral derivatives and similarity metrics to retrieve leaf biochemical traits from bidirectional reflectance. Remote Sens. Environ. 267, 112761. https://doi.org/10.1016/J.RSE.2021.112761.
Wan, L., Zhou, W., He, Y., Wanger, T.C., Cen, H., 2022. Combining transfer learning and hyperspectral reflectance analysis to assess leaf nitrogen concentration across different plant species datasets. Remote Sens. Environ. 269, 112826. https://doi.org/10.1016/J.RSE.2021.112826.
Wang, S., Guan, K., Wang, Z., Ainsworth, E.A., Zheng, T., Townsend, P.A., Liu, N., Nafziger, E., Masters, M.D., Li, K., Wu, G., Jiang, C., 2021. Airborne hyperspectral imaging of nitrogen deficiency on crop traits and yield of maize by machine learning and radiative transfer modeling. Int. J. Appl. Earth Observ. Geoinform. 105, 102617. https://doi.org/10.1016/j.jag.2021.102617.
Wang, S., Guan, K., Zhang, C., Jiang, C., Zhou, Q., Li, K., Qin, Z., Ainsworth, E.A., He, J., Wu, J., Schaefer, D., Gentry, L.E., Margenot, A.J., Herzberger, L., 2023b. Airborne hyperspectral imaging of cover crops through radiative transfer process-guided machine learning. Remote Sens. Environ. 285, 113386. https://doi.org/10.1016/J.RSE.2022.113386.
Wang, Z., Skidmore, A.K., Wang, T., Darvishzadeh, R., Hearne, J., 2015. Applicability of the PROSPECT model for estimating protein and cellulose + lignin in fresh leaves. Remote Sens. Environ. 168, 205–218. https://doi.org/10.1016/J.RSE.2015.07.007.
Wang, Z., Townsend, P.A., Schweiger, A.K., Couture, J.J., Singh, A., Hobbie, S.E., Cavender-Bares, J., 2019. Mapping foliar functional traits and their uncertainties across three years in a grassland experiment. Remote Sens. Environ. 221, 405–416. https://doi.org/10.1016/J.RSE.2018.11.016.
Wang, Z., Féret, J.B., Liu, N., Sun, Z., Yang, L., Geng, S., Zhang, H., Chlus, A., Kruger, E. L., Townsend, P.A., 2023a. Generality of leaf spectroscopic models for predicting key foliar functional traits across continents: a comparison between physically- and empirically-based approaches. Remote Sens. Environ. 293, 113614. https://doi.org/10.1016/J.RSE.2023.113614.
Wold, S., Ruhe, A., Wold, H., Dunn III, W.J., 1984. The collinearity problem in linear regression. The partial least squares (PLS) approach to generalized inverses. SIAM J. Sci. Stat. Comput. 5, 735–743. https://doi.org/10.1137/0905052.
Wold, S., Sjöström, M., Eriksson, L., 2001. PLS-regression: a basic tool of chemometrics. Chemom. Intel. Lab. Syst. 58, 109–130. https://doi.org/10.1016/S0169-7439(01)00155-1.
Wu, J., Chavana-Bryant, C., Prohaska, N., Serbin, S.P., Guan, K., Albert, L.P., Yang, X., van Leeuwen, W.J.D., Garnello, A.J., Martins, G., Malhi, Y., Gerard, F., Oliviera, R. C., Saleska, S.R., 2017. Convergence in relationships between leaf traits, spectra and age across diverse canopy environments and two contrasting tropical forests. New Phytol. 214, 1033–1048. https://doi.org/10.1111/NPH.14051.
Wu, S., Zeng, Y., Hao, D., Liu, Q., Li, J., Chen, X., Asrar, G.R., Yin, G., Wen, J., Yang, B., Zhu, P., Chen, M., 2021. Quantifying leaf optical properties with spectral invariants theory. Remote Sens. Environ. 253, 112131. https://doi.org/10.1016/J.RSE.2020.112131.
Xie, R., Darvishzadeh, R., Skidmore, A.K., Heurich, M., Holzwarth, S., Gara, T.W., Reusen, I., 2021. Mapping leaf area index in a mixed temperate forest using Fenix airborne hyperspectral data and Gaussian processes regression. Int. J. Appl. Earth Observ. Geoinform. 95, 102242. https://doi.org/10.1016/J.JAG.2020.102242.
Xu, M., Liu, R., Chen, J.M., Liu, Y., Shang, R., Ju, W., Wu, C., Huang, W., 2019. Retrieving leaf chlorophyll content using a matrix-based vegetation index combination approach. Remote Sens. Environ. 224, 60–73. https://doi.org/10.1016/J.RSE.2019.01.039.
Yan, Z., Guo, Z., Serbin, S.P., Song, G., Zhao, Y., Chen, Y., Wu, S., Wang, J., Wang, X., Li, J., Wang, B., Wu, Y., Su, Y., Wang, H., Rogers, A., Liu, L., Wu, J., 2021. Spectroscopy outperforms leaf trait relationships for predicting photosynthetic capacity across different forest types. New Phytol. 232, 134–147. https://doi.org/10.1111/NPH.17579.
Yang, X., Tang, J., Mustard, J.F., Wu, J., Zhao, K., Serbin, S., Lee, J.E., 2016. Seasonal variability of multiple leaf traits captured by leaf spectroscopy at two temperate deciduous forests. Remote Sens. Environ. 179, 1–12. https://doi.org/10.1016/J.RSE.2016.03.026.
Yendrek, C.R., Tomaz, T., Montes, C.M., Cao, Y., Morse, A.M., Brown, P.J., McIntyre, L. M., Leakey, A.D.B., Ainsworth, E.A., 2017. High-throughput phenotyping of maize leaf physiological and biochemical traits using hyperspectral reflectance. Plant Physiol. 173, 614–626. https://doi.org/10.1104/PP.16.01447.
Yuan, K., Zhu, Q., Riley, W.J., Li, F., Wu, H., 2022. Understanding and reducing the uncertainties of land surface energy flux partitioning within CMIP6 land models. Agric. For. Meteorol. 319, 108920. https://doi.org/10.1016/J.AGRFORMET.2022.108920.
Zeng, Y., Hao, D., Huete, A., Dechant, B., Berry, J., Chen, J.M., Joiner, J., Frankenberg, C., Bond-Lamberty, B., Ryu, Y., Xiao, J., Asrar, G.R., Chen, M., 2022. Optical vegetation indices for monitoring terrestrial ecosystems globally. Nature Rev. Earth Environ. 3, 477–493. https://doi.org/10.1038/s43017-022-00298-5.
Zhang, Y., Hui, J., Qin, Q., Sun, Y., Zhang, T., Sun, H., Li, M., 2021. Transfer-learning-based approach for leaf chlorophyll content estimation of winter wheat from hyperspectral data. Remote Sens. Environ. 267, 112724. https://doi.org/10.1016/J.RSE.2021.112724.
Zhao, Y., Han, S., Meng, Y., Feng, H., Li, Z., Chen, J., Song, X., Zhu, Y., Yang, G., 2022. Transfer-learning-based approach for yield prediction of winter wheat from planet data and SAFY model. Remote Sens. 14, 5474. https://doi.org/10.3390/RS14215474.
Zhu, Q., Li, F., Riley, W.J., Xu, L., Zhao, L., Yuan, K., Wu, H., Gong, J., Randerson, J., 2022. Building a machine learning surrogate model for wildfire activities within a global earth system model. Geosci. Model Dev. 15, 1899–1911. https://doi.org/10.5194/GMD-15-1899-2022.